



First-principles study of manganese-stabilized hafnia

I.V. Maznichenko^a, S. Ostanin^{b,*}, A. Ernst^b, I. Mertig^a

^a Martin-Luther-Universität Halle-Wittenberg, Institut für Physik, D-06099 Halle (Saale), Germany

^b Max-Planck-Institut für Mikrostrukturphysik, Weinberg 2, D-06120 Halle (Saale), Germany

ARTICLE INFO

Available online 3 December 2008

Keywords:

Ab initio calculation

Hafnia

Magnetic impurity

High- T_C ferromagnetism

ABSTRACT

We present a first-principles study of the electronic and magnetic properties of cubic hafnium dioxide stabilized by Mn. We find this material to be ferromagnetic and half-metallic, with the Mn-impurity electronic states lying in the band gap of hafnia for a wide range of manganese concentration. Our *ab initio* calculations, within the local spin-density approximation, demonstrate that Mn-doped hafnia may be ferromagnetic at 700 K while its high- T_C ferromagnetism is robust to the oxygen vacancy defects and to how the Mn impurities are distributed over the cation sublattice.

© 2008 Elsevier B.V. All rights reserved.

1. Introduction

For the last decade, a rich expertise has been built up on how to integrate ferromagnetism into semiconductor materials [1] and, therefore, to advance toward novel spintronics devices, which possess the ability both to generate and manipulate electronic spin at room temperature and above. As well as a high Curie temperature, T_C , a useful attribute for any appropriate spintronics material is a large difference between the majority and minority spin density of states at the Fermi energy so that it can act as the source of a spin injection. In the best-characterized dilute magnetic semiconductors (DMS), such as Ga(Mn)As, a variety of factors continue to keep the measured Curie temperature below 173 K [2]. For this reason and in the wake of theoretical predictions [3] that ZnO should become ferromagnetic when doped with a transition metal, most of the experimental studies are currently focusing on magnetic oxides. So far, the room temperature ferromagnetism was experimentally detected in thin films of cobalt doped TiO₂ [4], HfO₂ [5,6] and Cr-doped In₂O₃ [7]. However, the picture here is also complicated. For instance, Zn_{1-x}Mn_xO is not ferromagnetic unless additional hole doping is provided [3]. Regarding the Co-doped TiO₂ and HfO₂ ceramics, their magnetic properties are heavily dependent on the structure and defects [8,9]. The magnetic oxide-based materials suitable for spintronics are scarce, indeed. They must be easy to fabricate, stable, and compatible with conventional semiconductors and metals. Ostanin and coworkers [10] have recently predicted that Mn-stabilized cubic zirconia to be half-metallic and ferromagnetic at 500 K. ZrO₂ is well known both as a catalyst and as an imitation diamond. Besides, ZrO₂ is one of few high dielectric constant and

wide-gap insulators and is known to be thermally stable on SiGe and, therefore, it meets the criteria of spintronics. In ZrO₂, the concentration of manganese, x_{Mn} , can exceed 40% while the theoretically estimated T_C increases with x_{Mn} above room temperature when $x_{Mn} > 20\%$ [10]. For experimental verification, Clavel et al. [11] have synthesized the 5% Mn-doped ZrO₂ nanoparticles. It was found that the coexistence of Mn(II) and Mn(III), tends to antiferromagnetic interactions and that a higher oxidation state is more likely to support ferromagnetism. The theory [10] anticipates that the presence of Mn(IV) in Mn-ZrO₂ can keep $T_C > 300$ K.

In this paper, from the basis of state-of-the-art *ab initio* electronic structure calculations we propose that Mn-doped cubic HfO₂ matches extremely demanding spintronics criteria. Pure HfO₂ is being investigated as a high dielectric constant insulating gate for field effect transistor technology. Although the upper limit of solubility of manganese in hafnia is unknown, it might be compatible with that of Mn-ZrO₂. The fundamental nature of DMS and magnetic oxides is far from being well understood. We believe that magnetically doped ceramics such as Mn-HfO₂ provide an ideal opportunity for the study of ferromagnetism associated with the carrier mediated half-metallicity.

2. Calculation details

Our propositions are based on extensive density functional theory calculations, within the local density approximation (LDA) to the exchange-correlation energy. In principle, *ab initio* calculations should result in a parameter-free picture, and the conventional LDA has been proven reliable in predicting ground-state properties of metallic systems and semiconductors. There are numerous applications of the LDA to calculations of T_C in DMS (for a recent review, see Ref. [12] and references therein).

* Corresponding author. Tel.: +49 3455 558 652; fax: +49 3455 511 223.
E-mail address: sostanin@mpi-halle.mpg.de (S. Ostanin).

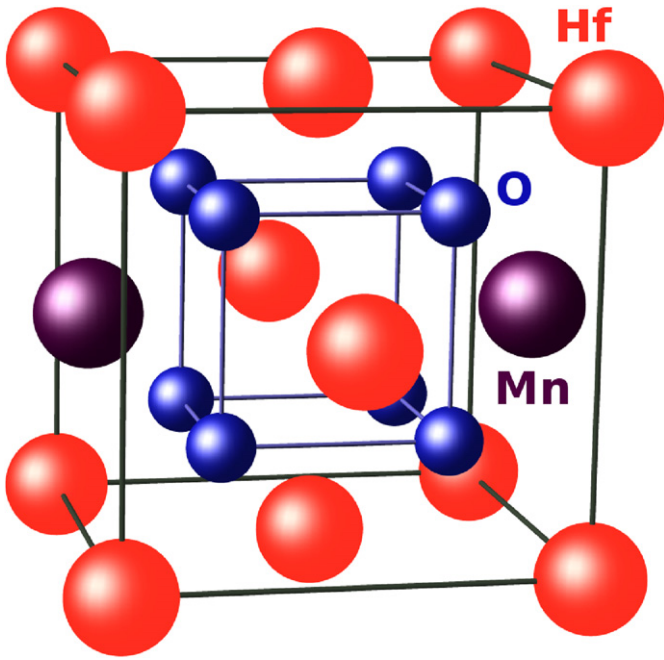


Fig. 1. The 12-atom fluorite supercell, $\text{Hf}_3\text{Mn}_1\text{O}_8$, corresponds to the 25% Mn– HfO_2 composition.

For DMS, a key issue is the energy position of the 3d states of a magnetic impurity. When the LDA tends to underestimate the localized character of the magnetic impurity states, the *ab initio* calculations are not entirely successful in describing all experimental findings and, therefore, much work is required to properly deal with the on-site Coulomb correlations in the framework of density functional theory. In particular, LDA+*U* [13] and the self-interaction-corrected (SIC) local spin-density approaches [14] can improve the picture of DMS [15,16]. For Mn-doped hafnia, the use of LDA was motivated by our previous experience with LDA+*U* calculations for Mn-doped zirconia [10], which demonstrate that the correlation effects cannot significantly change the magnetic properties of the material.

We use the multiple scattering Korringa–Kohn–Rostoker (KKR) theory, with the coherent-potential approximation (CPA) [17] to describe the motion of the electrons through the system. The CPA handles the location of the randomly distributed magnetic impurities. Alternatively, the effect of short-range order of impurities is studied using the 12-atom fluorite $\text{Hf}_3\text{Mn}_1\text{O}_8$ supercell, shown in Fig. 1, which corresponds to the 25% Mn– HfO_2 composition. The T_C value is extracted from the energy difference ΔE between total energies of the paramagnetic and ferromagnetic solutions: $k_B T_C = 2/3 \Delta E / x_{\text{Mn}}$. For the supercell modeling the 25% Mn– HfO_2 composition we estimated interatomic Heisenberg exchange parameters by applying the magnetic force theorem [18]. The obtained exchange parameters were used for the estimation of the Curie temperature within the random phase approximation (RPA) which should provide a better agreement with experiment [19,20].

3. Results and discussion

Using the KKR-CPA technique we computed, first, the equilibrium volume for several compositions of $\text{Hf}_{1-x}\text{Mn}_x\text{O}_2$ between $0 < x_{\text{Mn}} < 0.5$. The volume decreases with increasing x_{Mn} . In Fig. 2, we plot the calculated T_C versus x_{Mn} . T_C increases to well above

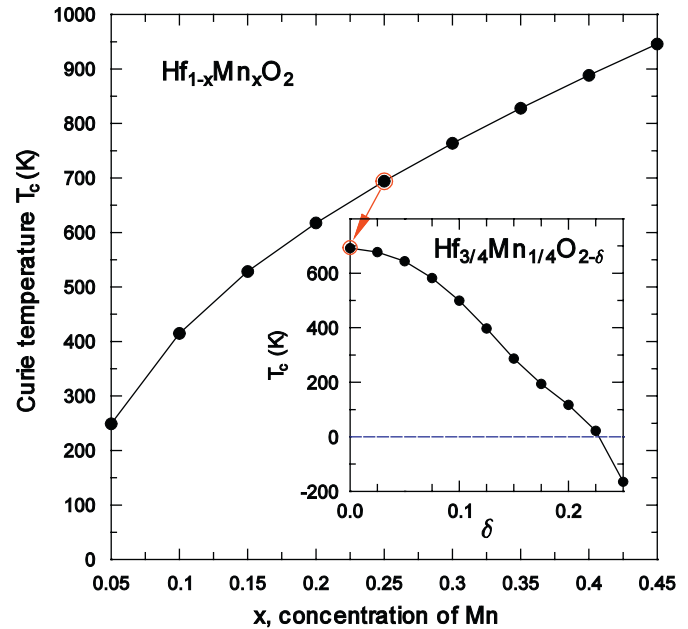


Fig. 2. Curie temperature upon Mn concentration in $\text{Hf}_{1-x}\text{Mn}_x\text{O}_2$, calculated for equilibrium volumes using the KKR-CPA method. Inset: The variation of T_C for $\text{Hf}_{3/4}\text{Mn}_{1/4}\text{O}_{2-\delta}$ as a function of the number of unrelaxed oxygen vacancies δ . The $\delta = 1/8$ accords with a half of the oxygen vacancy per manganese.

room temperature when $x > 5\%$. For Mn– ZrO_2 , the similar effect was found [10].

Surprisingly, in the case of Mn– HfO_2 we find that its Curie temperature increases more rapidly with the Mn concentration than that estimated for Mn-doped zirconia. In Mn– HfO_2 at $x = 0.25$ the estimated T_C is 694 K compared to 660 K which is predicted for Mn– ZrO_2 . At this concentration we calculated the interatomic Heisenberg exchange parameters by using magnetic force theorem [18] within a supercell approach. The estimated Curie temperature in the mean field approximation is 682 K and in a good agreement with the CPA result. This indicates that the CPA approximation is the appropriate tools to study the electronic structure of this material. Furthermore, the obtained exchange parameters were used for the calculation of the Curie temperature within the RPA [19,20]. The RPA is based on the Green function formalism for magnons and provides more reliable critical temperatures. For the 25% Mn– HfO_2 composition we found the RPA T_C to be 578 K. Since the RPA underestimates usually the critical temperature, we expect the experimental T_C to be between the RPA and mean field results.

Previously, Coey et al. [6] have reported that thin films of HfO_2 produced by pulsed-laser deposition on sapphire, yttria-stabilized ZrO_2 and silicon substrates show ferromagnetic magnetization curves with Curie temperature of the order of 400 K. Oxygen vacancy is the defect which is known to be presented in doped oxides. Until recently, the effect of the oxygen vacancy defects in ceramics on their possible high- T_C ferromagnetism was not studied. Here, we model the presence of oxygen vacancy in Mn– HfO_2 using the CPA. The inset of Fig. 2 illustrates the dependence of Curie temperature of 25% Mn– HfO_2 upon the number of oxygen vacancies δ . It is shown that the system is a room temperature ferromagnet when $\delta < 1/8$. It means that to keep T_C above 300 K the upper limit for the O vacancies accommodated in Mn– HfO_2 is one vacancy per two manganese atoms. Formally, it corresponds to Mn 3+ oxidation state. If $x_{\text{Mn}} < 0.25$ then the O vacancy limit becomes smaller. We suggest that the coexistence of Mn(IV) and Mn(III) in Mn-doped HfO_2 is essential for the issue of high T_C .

Another important property of magnetic oxide to be appropriate for spintronics is its half-metallicity. Our calculations clearly demonstrate that $\text{Zr}_{3/4}\text{Mn}_{1/4}\text{O}_2$ can obey such a behavior [10]. Fig. 3 shows the electronic density of states (DOS) calculated for the 25% Mn–HfO₂ composition, using both the supercell and CPA approaches. The spin-resolved DOS shows the metallic character for majority spin (Fig. 3a) and the band gap of ~1 eV for minority spin (Fig. 3b). Hence, the 25% Mn–HfO₂ as well as Mn-stabilized zirconia can be half-metallic at 0 K.

The lowest unoccupied electronic states for the minority spin channel of 25% Mn–HfO₂ are composed by the Mn 3d states, namely, the e_g and t_{2g} subbands, which are separated from each

other by the crystal field. Because of well known strong localization of the e_g and t_{2g} states, it is unlikely that the half-metallic behavior of Mn–HfO₂ can be significantly affected at the finite temperatures. This makes this material very appealing.

The Mn magnetic moments calculated for $x_{\text{Mn}} = 0.25$ using the CPA and supercell approaches are 3.35 and 3.41 μ_B , respectively. The total magnetization calculated per cell shows rather different values: 2.37 μ_B in the case of CPA and 2.99 μ_B when the 12-atom supercell is used. Hence, the induced magnetic moments are directed antiparallel to the Mn magnetic moment. It is clear that the widely used local CPA cannot properly treat the long-range interactions, which can play an important role in the system. The Mn magnetic moment weakly depends on x_{Mn} while it notably increases with the O vacancy concentration δ . For $x_{\text{Mn}} = 0.25$ and $\delta = 0.25$ we obtain 4.21 μ_B on the Mn site and 4.69 μ_B per cell. It seems that at the presence of unrelaxed oxygen vacancy in Mn–HfO₂ some induced magnetic moments being aligned parallel to the Mn moment, contribute to the total magnetic moment. The sign of the O magnetic moments is negative between $0 < \delta < 0.5$ and then it vanishes at $\delta = 0.5$ while the Mn moment adopts its integer value of 4 μ_B . However, in search for high- T_C Mn-doped oxide the researches must keep the number of oxygen vacancies below $\frac{1}{8}$.

4. Summary

From the *ab initio* basis of our work we anticipate that Mn-stabilized cubic hafnia, $\text{Hf}_{1-x}\text{Mn}_x\text{O}_{2-\delta}$, can become a room temperature half-metallic ferromagnet when $x_{\text{Mn}} > 0.2$ and $\delta < 0.125$. This means that the Mn/Hf ratio is larger than 1:5 and, simultaneously, the ratio between the number of possible oxygen vacancies and Mn impurities must be less than 1:2, providing the coexistence of Mn(IV) and Mn(III) in the system. Thus, we find the key electronic and structural factors for optimal magnetic doping of Mn–HfO₂.

Acknowledgement

This work was supported from the DFG SFB 762 “Funktionalität Oxidischer Grenzflächen”.

References

- [1] H. Ohno, Science 281 (1998) 951; S.A. Wolf, D.D. Awschalom, R.A. Buhrman, J.M. Daughton, S. von Molnár, M.L. Roukes, A.Y. Chtchelkanova, D.M. Treger, Science 294 (2001) 1488; F.J. Jedema, A.T. Filip, B.J. van Wees, Nature (London) 410 (2001) 345.
- [2] K.Y. Wang, R.P. Campion, K.W. Edmonds, M. Sawicki, T. Dietl, C.T. Foxon, B.L. Gallagher, in: J. Menéndez, C.G. Van de Walle (Eds.), Proceedings of the 27th International Conference on the Physics of Semiconductors, Springer, New York, 2005, p. 333.
- [3] T. Dietl, H. Ohno, F. Matsukura, J. Cibert, D. Ferrand, Science 287 (2000) 1019.
- [4] Y. Matsumoto, M. Murakami, T. Shono, T. Hasegawa, T. Fukumura, M. Kawasaki, P. Ahmet, T. Chikyow, S. Koshihara, H. Koinuma, Science 291 (2001) 854.
- [5] M. Venkatesan, C.B. Fitzgerald, J.M.D. Coey, Nature (London) 430 (2004) 630.
- [6] J.M.D. Coey, M. Venkatesan, C.B. Fitzgerald, Nat. Mater. 4 (2005) 173.
- [7] J. Philip, A. Punnoose, B.I. Kim, K.M. Reddy, S. Layne, J.O. Holmes, B. Satpati, P.R. LeClair, T.S. Santos, J.S. Moodera, Nat. Mater. 5 (2006) 298.
- [8] L.-H. Ye, A.J. Freeman, Phys. Rev. B 73 (2006) 081304(R).
- [9] C. Das Pemmaraju, S. Sanvito, Phys. Rev. Lett. 94 (2005) 217205.
- [10] S. Ostanin, A. Ernst, L.M. Sandratskii, P. Bruno, M. Däne, I.D. Hughes, J.B. Staunton, W. Hergert, I. Mertig, J. Kudrnovský, Phys. Rev. Lett. 98 (2007) 016101.
- [11] G. Clavel, M.-G. Willinger, D. Zitoun, N. Pinna, Eur. J. Inorg. Chem. 6 (2008) 863.
- [12] T. Jungwirth, J. Sinova, J. Mašek, J. Kučera, A.H. MacDonald, Rev. Mod. Phys. 78 (2006) 809.
- [13] V.I. Anisimov, F. Aryasetiawan, A.I. Lichtenstein, J. Phys.: Condens. Matter. 9 (1997) 767.

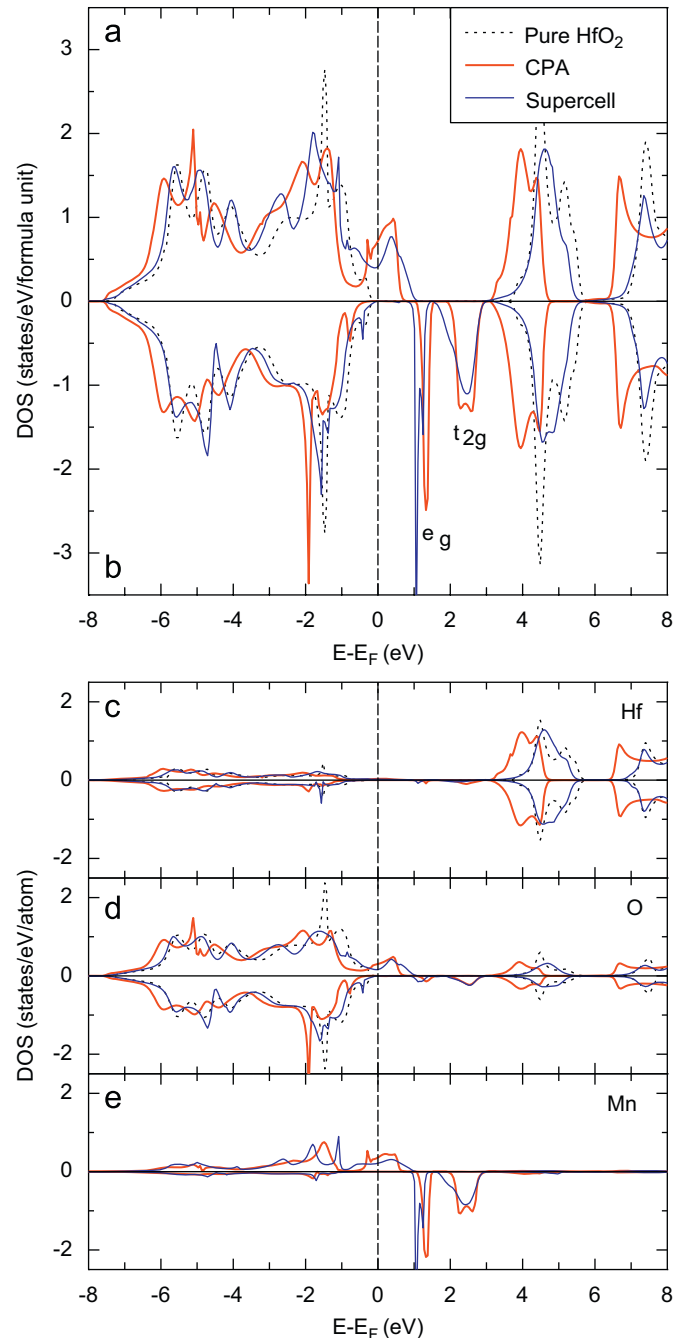


Fig. 3. (a), (b) Spin-resolved DOS of $\text{Hf}_{3/4}\text{Mn}_{1/4}\text{O}_2$, calculated using the supercell and CPA approaches. The DOS of pure HfO₂ is shown for comparison. (c)–(e) The corresponding site-resolved DOS curves.

- [14] J. Perdew, A. Zunger, *Phys. Rev. B* 23 (1981) 5048.
- [15] T.C. Schulthess, W.M. Temmerman, Z. Szotek, W.H. Butler, G.M. Stocks, *Nat. Mater.* 4 (2005) 838.
- [16] A. Ernst, L.M. Sandratskii, M. Bouhassoune, J. Henk, M. Lüders, *Phys. Rev. Lett.* 95 (2005) 237207.
- [17] G.M. Stocks, W.M. Temmerman, B.L. Gyorffy, *Phys. Rev. Lett.* 41 (1978) 339.
- [18] A.I. Liechtenstein, M.I. Katsnelson, V.P. Antropov, V.A. Gubanov, *J. Magn. Mater.* 67 (1987) 65.
- [19] J. Ruzs, I. Turek, M. Divis, *Phys. Rev. B* 71 (2005) 174408.
- [20] E. Sasioglu, L.M. Sandratskii, P. Bruno, *Phys. Rev. B* 72 (2005) 184415.